CCR7 deficiency modulates T cell response and increases susceptibility to *Yersinia pseudotuberculosis* infection

Joern Pezoldt[1#], Fabio Pisano[2#], Wiebke Heine[2], Maria Pasztoi[1], Maik Rosenheinrich[2], Aaron M. Nuss[2], Marina C. Pils[3], Immo Prinz[4], Reinhold Förster[4], Jochen Huehn[1#], Petra Dersch[2#*]

[1]Department of Experimental Immunology Helmholtz Centre for Infection Research, 38124 Braunschweig, Germany
[2]Department of Molecular Infection Biology, Helmholtz Centre for Infection Research, 38124 Braunschweig, Germany
[3]Mouse Pathology, Animal Experimental Unit, Helmholtz Centre for Infection Research, Braunschweig, Germany
[4]Institute for Immunology, Medical School Hannover, Hannover, Germany

[#]Equal contribution

*Corresponding author

Dept. of Molecular Infection Biology,
Helmholtz Centre for Infection Research
38124 Braunschweig, Germany
Phone: +49-531-6181-5700
FAX: +49-531-6181-5709
e-mail: petra.dersch@helmholtz-hzi.de

Short title: CCR7 strengthens immune response to *Yersinia*.

Keywords: *Yersinia pseudotuberculosis*, CCR7, dendritic cells, T cells, Peyer's Patches, mesenteric lymph nodes

Abstract (185 words)

Background: To successfully limit pathogen dissemination an immunological link between the entry tissue of the pathogen and the underlying secondary lymphoid organs (SLO) needs to be established to prime adaptive immune responses. Here, the prerequisite of CCR7 to mount host immune responses within SLOs during gastrointestinal *Yersinia pseudotuberculosis* infection to limit pathogen spread was investigated.

Methods: Survival, bacterial dissemination, intestinal and systemic pathology of wild type (WT) and CCR7$^{-/-}$ mice were assessed and correlated to the presence of immune cell subsets and cytokine responses throughout the course of infection.

Results: CCR7$^{-/-}$ mice show a significantly higher morbidity and are more prone to pathogen dissemination, intestinal and systemic inflammation during the oral route of infection. Significant impact of CCR7 deficiency over the course of infection on several immunological parameters were observed, i.e. elevated neutrophil-dominated innate immune response in Peyer's Patches, limited DC migration to mesenteric lymph nodes (mLNs) causing a reduced T cell-mediated adaptive immune responses (in particular Th17-like responses) in mLNs.

Conclusion: Our work indicates that CCR7 is required to mount a robust immune response against enteropathogenic *Y. pseudotuberculosis* by promoting Th17-like responses in mLNs.

Introduction (3335 words)

Immune cell migration processes during homeostatic and inflammatory conditions are regulated by chemokines and their receptors [1, 2]. Migration is key to mitigate pathogen-specific signals from peripheral tissues, like the intestine, to secondary lymphoid organs (SLO) such as mLNs, a process essential for fast, efficient and pathogen-specific immune responses [3]. This migration is dependent on the expression of chemokine receptors (CCR), such as CCR7. CCR7 is particularly important for the migration of certain immune cells, i.e. DCs, monocytes and T cells to Peyer's Patches (PPs) and mLNs [3, 4]. CC-chemokine ligand 19 (CCL19) and CCL21 are the ligands for CCR7 and are expressed by stromal cells located in the T cell zone of SLOs and afferent lymphatic cells [5-9]. Different from other chemokines, their expression is constitutive rather than inflammation-dependent, allowing entry of T cells from blood or peripheral tissues via high endothelial venules or lymphatics [3, 10]. Antigen presenting cells (APCs), such as DCs, increase CCR7 surface expression upon activation, which enhances their migration to SLOs [11, 12], and respective priming of pathogen-tailored immune responses [13]. Consequently, a deficiency of CCR7 leads to impaired DC migration and T cell homing into draining lymph nodes [14].

Despite its key role in triggering adaptive immune responses, no considerable abrogation of protective responses against several tested viral and bacterial pathogens has been observed in CCR7-deficient ($CCR7^{-/-}$) mice [15-17]. However, upon cutaneous infection by *Leishmania major*, CCR7-dependent monocyte migration is required for protection, since $CCR7^{-/-}$ mice are not able to clear the pathogen and develop a chronic cutaneous infection [4].

77 Other pathogens such as *Salmonella enterica* serovar Typhimurium and
78 *Listeria monocytogenes* are able to exploit CCR7-dependent migration of
79 APCs to co-migrate to the draining lymph nodes in a Trojan-horse fashion
80 upon oral infection [18-20].

81 *Y. pseudotuberculosis* causes several gut-associated diseases ranging
82 from self-limiting enteritis and abdominal pain to autoimmune disorders such
83 as reactive arthritis [21]. Upon ingestion of contaminated food or water,
84 *Y. pseudotuberculosis* efficiently transmigrates through the intestinal epithe-
85 lium of the ileum and colonizes PPs, mLNs, and at later stages also systemic
86 organs such as liver and spleen [22]. Whether CCR7-mediated migration is
87 essential for mounting effective immune responses against *Y. pseudotubercu-*
88 *losis* has not been investigated to date. However, recent work showed that
89 enteropathogenic *Y. enterocolitica* induces expression of CCR7 on lamina
90 propria $CD103^+$ DCs [23].

91 In the present study, we employed a sub-lethal oral infection model for
92 *Y. pseudotuberculosis* and observed that $CCR7^{-/-}$ mice were not able to
93 contain bacterial dissemination. Surprisingly, $CCR7^{-/-}$ mice succumbed to
94 infection, implying a protective role of CCR7 to primary infections with
95 *Y. pseudotuberculosis* by promoting tissue-tailored immune reactions,
96 potentially mediating the robust induction of protective T cell responses in
97 mLNs.
98

Materials and Methods

In the present study, the *Y. pseudotuberculosis* strain IP32953 was employed in all experiments [24]. All detailed information about material and methods, i.e. the histology and cytokine expression analysis, mouse infections, flow cytometry analysis and the statistical analyses are given in the methods section of the supplementary materials.

Ethics statement

All animal work was performed in strict accordance with the German Recommendations of the Society for Laboratory Animal Science (GV-SOLAS) and the European Health Recommendations of the Federation of Laboratory Animal Science Associations (FELASA). The animal protocol was approved by the Niedersächsisches Landesamt für Verbraucherschutz und Lebensmittelsicherheit: animal licensing committee permission no. 33.9.42502-04-055/09 and 33.9.42502-04-13/1166. Animals were handled with appropriate care and welfare, and all efforts were made to minimize suffering.

Results

CCR7 deficiency increases susceptibility to oral but not to intravenous *Y. pseudotuberculosis* infection

In order to dissect the impact of CCR7 functionality on the infection route-dependent virulence of *Y. pseudotuberculosis*, WT and CCR7$^{-/-}$ mice were infected orally or intravenously. Weight and health status were monitored for up to 20 days. Although oral infection with a lethal dose of 10^7 CFUs showed only a minor difference in lethality rates, infection with a sub-lethal dose of

10^6 CFUs resulted in high mortality rates solely for CCR7$^{-/-}$ mice (**Figure 1**). Systemic intravenous application with 10^3 or 10^4 CFUs resulted in rapid dose-dependent lethality, but no differences could be observed between WT and CCR7$^{-/-}$ animals, whereas survival of mice infected with 10^2 CFUs was not affected by the infection (**Figure 1**). These results underline that CCR7-dependent mechanisms are only required in the context of the natural oral route of infection, involving a progression of *Y. pseudotuberculosis* through the intestine.

CCR7 sufficiency limits bacterial replication and dissemination

Systemic dissemination of the pathogen and its uncontrolled replication in organs such as liver and spleen are the driving force behind lethality of gastrointestinal infections. The similarity between host infiltration mechanisms triggered by enteric pathogens such as *Salmonellae* and *Yersiniae* [25], prompted us to assess whether CCR7 functionality has an impact on *Y. pseudotuberculosis* dissemination from the intestine to mLNs and systemic organs such as liver and spleen. Thereto, WT and CCR7$^{-/-}$ mice were orally infected with 10^6 CFUs of *Y. pseudotuberculosis* and sacrificed 3, 5 and 7 days post infection, and the bacterial load of infected tissues was assessed. As shown in **Figure 2A-B**, overall colonisation levels within small intestines, mLNs and systemic organs were significantly higher in CCR7$^{-/-}$ mice as compared to WT controls. The bacterial titre in all tested host tissues was already high at day 3 post infection and remained at high levels over the course of infection. In contrast, a significant decrease of bacterial load was monitored in WT mice, in particular in gut-associated tissues (**Figure 2A-B**).

In summary, CCR7$^{-/-}$ mice show a rapid colonisation of intestinal tissues and systemic organs already early during the infection when compared to WT animals, which are also more proficient in eliminating the pathogen during the course of infection. Our results indicate that *Y. pseudotuberculosis* does not rely on CCR7-mediated migration for dissemination and that CCR7 is beneficial to the host limiting pathogen expansion in the context of the natural oral route of infection.

CCR7 deficiency results in severe intestinal and systemic inflammation during *Y. pseudotuberculosis* infection

In order to determine the course and extent of inflammation and pathology, WT and CCR7$^{-/-}$ mice were infected with *Y. pseudotuberculosis* and intestinal and systemic organs were assessed for organ integrity and level of inflammation by H & E staining. As previously reported [26], small intestines of CCR7$^{-/-}$ mice contained smaller PPs displaying an altered architecture compared to WT animals (**Figure 3**). Lack of CCR7 resulted in increased inflammation both in PPs and lamina propria at all time points assessed after infection, resulting in an extensive influx of macrophages and neutrophils, and subsequent swelling of PPs (**Figure 3**). Additionally, within PPs pro-inflammatory cytokines interleukin (IL)-6, interferon (IFN)-γ and tumor-necrosis factor (TNF)-α were highly upregulated in CCR7$^{-/-}$ as compared to WT mice (**Supplementary Figure 1**). As early as day 3 post infection, macrophage infiltration strongly increased in mLNs of CCR7$^{-/-}$ compared to WT mice (**Figure 3**). WT spleens showed early hyperplasia already on day 3 post infection, increasing from day 5 to day 7. CCR7$^{-/-}$ spleens showed marked

necrosis and numerous *Yersinia* colonies, whereas most WT organs did not (**Figure 3**). Additionally, white pulps of CCR7$^{-/-}$ spleens were smaller in size compared to WT controls in the uninfected state and also throughout the infection (**Figure 3**). Inflammation and bacterial load within livers of WT mice decreased on day 7 compared to earlier stages of infection, but CCR7$^{-/-}$ livers lastingly showed elevated levels of bacteria and inflammation (**Figure 2B**, data not shown).

Taken together, the histological data confirm that the majority of WT animals control the infection in the small intestine. Dissemination to mLNs, spleen and liver and accompanying systemic inflammation is limited (**Supplemental Figure 2**). In contrast, infection of CCR7$^{-/-}$ mice results in an extensive lymphatic and systemic dissemination of *Yersiniae* and triggers a rapid and sustained inflammation of infected tissues.

CCR7 deficiency impacts myeloid cell composition during infection to a minor extent

To assess concomitant cellular effects based on CCR7-deficiency that might dominate the immune response and account for the strong pro-inflammatory environment in PPs of CCR7$^{-/-}$ mice, we quantified changes to the myeloid compartment 1 and 5 days after infection with 10^6 CFU of *Y. pseudotuberculosis* in PPs and mLNs using flow cytometry (gating strategy in **Supplementary Figure 3A**). Already under steady state conditions, PPs and mLNs of CCR7$^{-/-}$ mice were characterised by significant higher numbers of CD11b$^+$Ly6G$^+$ neutrophils in intestinal tissues, indicating elevated inflammation in the CCR7$^{-/-}$ animals (**Figure 4**). Absolute numbers of monocytes and

199 macrophages increased to a similar extent over the course of infection in both
200 WT and CCR7$^{-/-}$ mice, whereas the number of CD11b^{+}Ly6G^{+} neutrophils was
201 substantially higher in PPs of CCR7$^{-/-}$ mice at all time points assessed
202 (**Figure 4**). In addition, slightly higher numbers of monocytes (CD11b^{+}Ly6C^{high}
203 and CD11b^{+}Ly6C^{-}), but not macrophages (F4/80^{+}) were observed in PPs of
204 CCR7$^{-/-}$ mice at day 1 post infection. No major impact of CCR7 on the myeloid
205 cell composition was observed for the spleen (**Supplementary Figure 3B**). In
206 summary, high numbers of professional phagocytes in PPs and mLNs in
207 CCR7$^{-/-}$ mice at the initial stage of infection indicate an aptitude for inflamma-
208 tory responses.
209
210 **CCR7 sufficiency promotes effective migration of professional antigen-**
211 **presenting cells to mLNs**
212 Based on the primary observation that CCR7 deficiency results in high letha-
213 lity only in the context of the natural oral route of infection at late stage 7 days
214 post infection, we assumed that the lack of successful priming of the adaptive
215 immune system might drive fatalities. Antigen presentation to T cells relies on
216 migration of activated and pathogen-antigen loaded APCs from the periphery
217 to draining lymph nodes, a process that relies on CCR7 expression [26]. In
218 contrast to respiratory tract infections with *P. aeruginosa*, where CCR7$^{-/-}$ mice
219 are more proficient in eliminating the pathogen [17], we observed that CCR7
220 expression is important for host survival (**Figure 1**).
221 In order to test whether CCR7-dependent migration of DCs takes place
222 during *Y. pseudotuberculosis* infection, WT and CCR7$^{-/-}$ mice were orally
223 challenged with 10^{7} CFUs of the pathogen and the cellular composition of

CD11c^{+}MHCII^{+} DCs in mLNs was assessed via flow cytometry 3 and 5 days post infection (gating strategy in **Supplementary Figure 4**). As expected, mLNs of uninfected CCR7$^{-/-}$ mice already presented significantly lower numbers of CD11c^{+}MHCII^{+} DCs in comparison to WT controls (**Figure 5A-B**). Three days after infection, an increase in the frequency of CD11c^{+}MHCII^{+} DCs was observed in both groups, however the number of DCs dropped back to initial levels in CCR7$^{-/-}$ mLNs on day 5 post infection, while the number of DCs remained stable over the course of infection in WT mice (**Figure 5B**). Importantly, the frequency of T cells was unaffected in WT mice, while a significant reduction in T cell abundance was observed at day 5 post infection in CCR7$^{-/-}$ mice (**Figure 5C**).

Together, the monitoring of DCs and T cells during the course of *Y. pseudotuberculosis* infection confirms the CCR7-dependent influx of activated DCs into mLNs, potentially priming adaptive immune responses and sustaining the pool of T cells.

CCR7 deficiency limits effector T cell cytokine responses in mLNs

The predisposition of CCR7$^{-/-}$ mice to mount a rapid neutrophil response limited DC migration to the mLNs and reduced abundance of T cells at day 5 post infection tempted us to assess whether T cell responses are negatively impacted by the innate immunity dominated responses in CCR7$^{-/-}$ mice. To this end, we performed cytokine expression analysis of the mLNs to monitor cytokine responses during the infection. Pro-inflammatory cytokines including IL-6, IFN-γ and TNF-α were expressed to a similar extent in mLN for both CCR7$^{-/-}$ and WT mice (**Figure 6A**). However, only WT, but not CCR7$^{-/-}$ mice

displayed a robust upregulation of Th17-like response cytokines IL-17A, IL-17F and IL-21 at day 5 post infection in the mLNs (**Figure 6B**), which is in line with the sustained abundance of DCs in the WT animals (**Figure 5B**). Notably, the cytokine response in WT animals is heterogenous with Th17- or Th2-like cytokine responses aggregating per mouse (**Figure 6C**). This correlated with a bimodal distribution of RORγT$^+$ cells within the CD3$^+$CD4$^+$ in the mLNs (**Figure 6D**). To further evaluate, whether observed upregulation of IL-17A and IL-17F in some of the WT mice is required to defeat the infection, we performed oral infections with a lethal dose of 10^7 CFU in WT and double knockout mice for IL-17A and IL-17F (*Il17af*$^{-/-}$). As shown in **Figure 6D**, we observed that IL-17A/F sufficiency allowed survival of a significant proportion of mice.

In summary, the time-course profiling of T cell response cytokines showed that specific immune responses and in particular Th17-like responses are initiated and sustained in mLNs of WT, whereas CCR7$^{-/-}$ mice are not able to establish a supportive microenvironment for effector T cell responses in the mLN irrespective of the common strong Th1-like response in both WT and CCR7$^{-/-}$ mice (Figure **6A-B**).

Discussion

The follicle-associated epithelium of PPs contains high numbers of M cells that serve as main entry sites for enteropathogenic *Yersiniae*. Subsequent colonization of PPs serves as a staging ground for spread via lymph and/or blood into mLNs, liver and spleen [27]. Enteropathogenic *Yersiniae* were shown to be in close contact with mononuclear phagocytes and dendritic cells

[23]. This indicated that they could serve as alternative front gate for *Yersinia* into the lamina propria and as transport vehicles via blood/lymph to mLNs and deeper organs.

Here, we addressed the role of CCR7-dependent migration of immune cells to PPs and mLNs for *Y. pseudotuberculosis* virulence. CCR7 is up-regulated in DCs upon contact with inflammatory or tissue-damaging molecules, and this initiates homing of DCs from peripheral to lymphoid tissue to trigger an adaptive immune response [3, 7, 14]. Although CCR7 is also up-regulated on DCs as response to *Y. pseudotuberculosis* infection, we found that its absence does not reduce dissemination of this pathogen. In contrast, CCR7 deficiency enables a more efficient proliferation and dissemination of *Y. pseudotuberculosis* in host tissue and renders the host more susceptible to a natural oral infection. Notably, CCR7 competence had no impact on host responses in case of intravenous *Y. pseudotuberculosis* infection. This illustrates that the entry route is critical for the impact of CCR7-dependent migrations and adaptation of the immune system to limit *Y. pseudotuberculosis* dissemination to deeper tissues. In this context, previous studies reporting that CCR7 has no or only limited influence on successful host responses in case of non-physiological intravenous *L. monocytogenes* and LCMV (Lymphocytic choriomeningitis virus) infection [15, 16] should be re-evaluated.

In contrast to what has been reported for *Y. enterocolitica* and *Salmonella* Typhimurium [18, 20, 23, 28], we observed that systemic dissemination of *Y. pseudotuberculosis* does not require CCR7-dependent migration of DCs and monocytes. The reason for this remains elusive, but it is possible that a

299 set of different *Yersinia* surface adhesins/invasins and/or secreted factors
300 enables the pathogen to actively enter deeper tissues and follow distinct
301 dissemination pathways independent of immune cell migration. One study
302 documented that colonisation of draining lymph nodes by *Y. pestis* occurred
303 due to trafficking of infected DCs/monocytes in response to redundant chemo-
304 tactic signals, including CCR7 [28]. However, a new method studying
305 *Y. pestis* transmission by its natural route (i.e. the bite of an infected flea)
306 demonstrated that, although professional phagocytes quickly migrate to bite
307 sites and interact with bacteria, migration to lymph nodes appeared to be
308 independent of CCR7 [29, 30]. Similar to *Y. pseudotuberculosis*, CCR7 ex-
309 pression is also elevated in *Y. pestis*-infected DCs, but bacterial components
310 encoded on the *Yersinia* virulence plasmid seems to abolish migration of DCs
311 to the draining lymph nodes [31].
312 Our results show that CCR7 competence restricts *Y. pseudotuberculosis*
313 dissemination and systemic organ burden especially later during infection.
314 They also indicate that the observed impact of CCR7 on the host response to
315 *Yersinia* depends on the specific environment encountered within host tissue
316 during the course of infection. It is known that different immune alterations are
317 associated with $CCR7^{-/-}$ deficiency and these changes may alter the
318 behaviour of the pathogen. An additional detriment is the lack of development
319 of oral tolerance relying on tolerogenic intestinal antigen-bearing DCs [32],
320 and establishment of humoral immune responses [33]. These limitations to
321 develop balanced intestinal immunity potentially drive chronic inflammation,
322 alter myeloid cell composition, and result in elevated levels of neutrophils and
323 inflammatory monocytes under steady state conditions.

Moreover, PPs of CCR7-deficient mice are scarce in naïve $CD4^+$ T cells [34]. Deficiencies in adaptive immunity were shown to promote adverse small intestinal Th17 responses that drive inflammation and disease progression [35, 36]. In line with exacerbated inflammation, we observed rapid swelling of PPs in $CCR7^{-/-}$ mice upon infection, reaching maximal size on day 5 to 7, when $CCR7^{-/-}$ mice succumbed to disease. The major influx of neutrophils and inflammatory monocytes could be mediated by a positive autocrine feedback loop. As neutrophils are highly abundant in $CCR7^{-/-}$ mice, incoming *Y. pseudotuberculosis* are recognized by a larger pool of neutrophils, elevating the secretion of CXCR2 ligands by neutrophils, actively promoting further accumulation of $CXCR2^+$ neutrophils and monocytes [2, 37]. The elevated presence and influx of neutrophils could shift the inflammatory metabolic environment, increase pathogen-targeted immune responses and inflammation and drive observed pathogenesis in $CCR7^{-/-}$ PPs [38, 39]. Furthermore, $CCR7^{-/-}$ mice are marked by a sustained pro-inflammatory immune response in PPs. However, they do not seem able to establish a cytokine milieu in the mLN in response to a *Yersinia* infection, which promote effector T cell responses, such as the induction of sufficient IL-2 levels supporting the expanding T cell population [40]. mLNs of $CCR7^{-/-}$ mice are characterized by an influx of DCs early during infection, but are not able to sustain the DC compartment later during infection. This early influx of DCs in $CCR7^{-/-}$ mice is potentially due to blood-derived DC precursors, as a response to the inflammation [41]. This indicated that the migration of DCs from the intestine to the mLNs is required to promote T cell differentiation and Th17-like immunity in the context of a *Y. pseudotuberculosis* infection. The source of IL-

17 is challenging to determine as several cellular entities, e.g. T cells and innate lymphoid cells, can contribute to Th17-like immune responses [42]. Notably, a recent work investigating infections with *Y. pestis* revealed that neutrophils are the main source of IL-17A in the lymph nodes. This study also demonstrated that IL-17A produced by neutrophils protects against pneumonic plague through orchestrating IFN-γ activated macrophage programming [43]. In fact, abrogation of IL-17AF significantly aggravated the infection, similar to *Y. pestis*, indicating that IL-17A is also a critical requirement for early protection of a *Y. pseudotuberculosis* infection. Thus, increased abundance of neutrophils in CCR7$^{-/-}$ mice could also contribute to the protective effect through IL-17A production.

Our data underline specific host-pathogen interactions during infection and emphasize the importance to utilize infection models with the evolved route of infection to truly dissect tissue-specific requirements for immune responses. In case of oral *Y. pseudotuberculosis* infection, the chemokine receptor CCR7 seems to be required to mount proper T cell immune responses to limit pathogen dissemination and ensure host survival.

Supplementary data

Supplementary Figures and Methods will be made available at http://jid.oxfordjournal.org. Consisting of data provided by the author to benefit the reader, the posted materials are not copyedited and are the sole responsibility of the author, so questions and comments should be addressed to the author.

Funding. This work was supported by the Deutsche Forschungsgemeinschaft (SFB621, Project B10), the Hannover Biomedical Research School (HBRS), the Center for Infection Biology (ZIB), a stipend of the IRTG1273 funded by the Deutsche Forschungsgemeinschaft given to Maik Rosenheinrich and a stipend of the HZI Graduate School given to Wiebke Heine. Petra Dersch is supported by the Deutsches Zentrum für Infektionsforschung (DZIF).

Acknowledgment. We thank Martin Fenner for discussions and Tanja Krause, Karin Paduch, and Maria Ebel for technical assistance.

Foot Note Page

Potential conflicts of interest. All authors: No reported conflicts. All authors have submitted the ICMJE Form for Disclosure of Potential Conflicts of Interest. Conflicts that the editors consider relevant to the content of the manuscript have been disclosed.

Presentation of data. The presented information has not previously been presented at a national or international meeting.

References

1. Sallusto F, Baggiolini M. Chemokines and leukocyte traffic. Nat Immunol **2008**; 9:949-52.

2. Griffith JW, Sokol CL, Luster AD. Chemokines and chemokine receptors: positioning cells for host defense and immunity. Annu Rev Immunol **2014**; 32:659-702.

3. Forster R, Davalos-Misslitz AC, Rot A. CCR7 and its ligands: balancing immunity and tolerance. Nat Rev Immunol **2008**; 8:362-71.

4. Kling JC, Mack M, Korner H. The absence of CCR7 results in dysregulated monocyte migration and immunosuppression facilitating chronic cutaneous leishmaniasis. PLoS One **2013**; 8:e79098.

5. Sozzani S. Dendritic cell trafficking: more than just chemokines. Cytokine Growth Factor Rev **2005**; 16:581-92.

6. Muller G, Hopken UE, Lipp M. The impact of CCR7 and CXCR5 on lymphoid organ development and systemic immunity. Immunol Rev **2003**; 195:117-35.

7. Jang MH, Sougawa N, Tanaka T, et al. CCR7 is critically important for migration of dendritic cells in intestinal lamina propria to mesenteric lymph nodes. J Immunol **2006**; 176:803-10.

8. Ohl L, Mohaupt M, Czeloth N, et al. CCR7 governs skin dendritic cell migration under inflammatory and steady-state conditions. Immunity **2004**; 21:279-88.

9. MartIn-Fontecha A, Sebastiani S, Hopken UE, et al. Regulation of dendritic cell migration to the draining lymph node: impact on T lymphocyte traffic and priming. J Exp Med **2003**; 198:615-21.

10. Rot A, von Andrian UH. Chemokines in innate and adaptive host defense: basic chemokinese grammar for immune cells. Annu Rev Immunol **2004**; 22:891-928.

422 11. Yanagihara S, Komura E, Nagafune J, Watarai H, Yamaguchi Y.
423 EBI1/CCR7 is a new member of dendritic cell chemokine receptor that is
424 up-regulated upon maturation. J Immunol **1998**; 161:3096-102.
425 12. Dieu MC, Vanbervliet B, Vicari A, et al. Selective recruitment of immature
426 and mature dendritic cells by distinct chemokines expressed in different
427 anatomic sites. J Exp Med **1998**; 188:373-86.
428 13. Guermonprez P, Valladeau J, Zitvogel L, Thery C, Amigorena S. Antigen
429 presentation and T cell stimulation by dendritic cells. Annu Rev Immunol
430 **2002**; 20:621-67.
431 14. Forster R, Schubel A, Breitfeld D, et al. Pillars Article: CCR7 Coordinates
432 the primary immune response by establishing functional
433 microenvironments in secondary lymphoid organs. Cell. 1999. 99: 23-33.
434 J Immunol **2016**; 196:5-15.
435 15. Junt T, Nakano H, Dumrese T, et al. Antiviral immune responses in the
436 absence of organized lymphoid T cell zones in plt/plt mice. J Immunol
437 **2002**; 168:6032-40.
438 16. Kursar M, Hopken UE, Koch M, et al. Differential requirements for the
439 chemokine receptor CCR7 in T cell activation during *Listeria*
440 *monocytogenes* infection. J Exp Med **2005**; 201:1447-57.
441 17. Eppert BL, Motz GT, Wortham BW, Flury JL, Borchers MT. CCR7
442 deficiency leads to leukocyte activation and increased clearance in
443 response to pulmonary *Pseudomonas aeruginosa* infection. Infect Immun
444 **2010**; 78:2099-107.
445 18. Voedisch S, Koenecke C, David S, et al. Mesenteric lymph nodes confine
446 dendritic cell-mediated dissemination of *Salmonella enterica* serovar

447 Typhimurium and limit systemic disease in mice. Infect Immun **2009**;
448 77:3170-80.
449 19. Pron B, Boumaila C, Jaubert F, et al. Dendritic cells are early cellular
450 targets of *Listeria monocytogenes* after intestinal delivery and are
451 involved in bacterial spread in the host. Cell Microbiol **2001**; 3:331-40.
452 20. Kaiser P, Slack E, Grant AJ, Hardt WD, Regoes RR. Lymph node
453 colonization dynamics after oral *Salmonella* Typhimurium infection in
454 mice. PLoS Pathog **2013**; 9:e1003532.
455 21. Dube P. Interaction of *Yersinia* with the gut: mechanisms of pathogenesis
456 and immune evasion. Curr Top Microbiol Immunol **2009**; 337:61-91.
457 22. Barnes PD, Bergman MA, Mecsas J, Isberg RR. *Yersinia*
458 *pseudotuberculosis* disseminates directly from a replicating bacterial pool
459 in the intestine. J Exp Med **2006**; 203:1591-601.
460 23. Drechsler-Hake D, Alamir H, Hahn J, et al. Mononuclear phagocytes
461 contribute to intestinal invasion and dissemination of *Yersinia*
462 *enterocolitica*. Int J Med Microbiol **2016**.
463 24. Chain PS, Carniel E, Larimer FW, et al. Insights into the evolution of
464 *Yersinia pestis* through whole-genome comparison with *Yersinia*
465 *pseudotuberculosis*. Proc Natl Acad Sci U S A **2004**; 101:13826-31.
466 25. Reis RS, Horn F. Enteropathogenic *Escherichia coli, Samonella, Shigella*
467 and *Yersinia*: cellular aspects of host-bacteria interactions in enteric
468 diseases. Gut Pathog **2010**; 2:8.
469 26. Forster R, Schubel A, Breitfeld D, et al. CCR7 coordinates the primary
470 immune response by establishing functional microenvironments in
471 secondary lymphoid organs. Cell **1999**; 99:23-33.

27. Carter PB. Animal model of human disease. *Yersinia enteritis*. Animal model: oral *Yersinia enterocolitica* infection of mice. Am J Pathol **1975**; 81:703-6.
28. St John AL, Ang WX, Huang MN, et al. S1P-dependent trafficking of intracellular *Yersinia pestis* through lymph nodes establishes buboes and systemic infection. Immunity **2014**; 41:440-50.
29. Shannon JG, Hasenkrug AM, Dorward DW, Nair V, Carmody AB, Hinnebusch BJ. *Yersinia pestis* subverts the dermal neutrophil response in a mouse model of bubonic plague. MBio **2013**; 4:e00170-13.
30. Shannon JG, Bosio CF, Hinnebusch BJ. Dermal neutrophil, macrophage and dendritic cell responses to Yersinia pestis transmitted by fleas. PLoS Pathog **2015**; 11:e1004734.
31. Velan B, Bar-Haim E, Zauberman A, Mamroud E, Shafferman A, Cohen S. Discordance in the effects of *Yersinia pestis* on the dendritic cell functions manifested by induction of maturation and paralysis of migration. Infect Immun **2006**; 74:6365-76.
32. Worbs T, Bode U, Yan S, et al. Oral tolerance originates in the intestinal immune system and relies on antigen carriage by dendritic cells. J Exp Med **2006**; 203:519-27.
33. Scandella E, Fink K, Junt T, et al. Dendritic cell-independent B cell activation during acute virus infection: a role for early CCR7-driven B-T helper cell collaboration. J Immunol **2007**; 178:1468-76.
34. Pabst O, Herbrand H, Friedrichsen M, et al. Adaptation of solitary intestinal lymphoid tissue in response to microbiota and chemokine receptor CCR7 signaling. J Immunol **2006**; 177:6824-32.

497 35. Littman DR, Pamer EG. Role of the commensal microbiota in normal and
498 pathogenic host immune responses. Cell Host Microbe **2011**; 10:311-23.
499 36. Bi Y, Liu G, Yang R. Reciprocal modulation between TH17 and other
500 helper T cell lineages. J Cell Physiol **2011**; 226:8-13.
501 37. Chou RC, Kim ND, Sadik CD, et al. Lipid-cytokine-chemokine cascade
502 drives neutrophil recruitment in a murine model of inflammatory arthritis.
503 Immunity **2010**; 33:266-78.
504 38. Kominsky DJ, Campbell EL, Colgan SP. Metabolic shifts in immunity and
505 inflammation. J Immunol **2010**; 184:4062-8.
506 39. Mumy KL, McCormick BA. The role of neutrophils in the event of intestinal
507 inflammation. Curr Opin Pharmacol **2009**; 9:697-701.
508 40. Boyman O, Sprent J. The role of interleukin-2 during homeostasis and
509 activation of the immune system. Nat Rev Immunol **2012**; 12:180-90.
510 41. Alvarez D, Vollmann EH, von Andrian UH. Mechanisms and
511 consequences of dendritic cell migration. Immunity **2008**; 29:325-42.
512 42. Hepworth MR, Monticelli LA, Fung TC, et al. Innate lymphoid cells
513 regulate CD4 T-cell responses to intestinal commensal bacteria. Nature
514 **2013**.
515 43. Bi Y, Zhou J, Yang H, et al. IL-17A produced by neutrophils protects
516 against pneumonic plague through orchestrating IFN-gamma-activated
517 macrophage programming. J Immunol **2014**; 192:704-13.
518
519

Figure Legends

Figure 1. CCR7 deficiency increases susceptibility to *Y. pseudotuberculosis* infection. WT and CCR7$^{-/-}$ mice were orally or intravenously infected with indicated CFUs of IP32953 and monitored over a period of up to 20 days. Data represents two to three independent experiments (n = 4-5 per experiment). Statistical analysis was performed with log-rank test (*** P<0.001).

Figure 2. CCR7 deficiency enhances bacterial replication and dissemination. WT and CCR7$^{-/-}$ were orally infected with 10^6 CFU of IP32953. The bacterial colonization was assessed 3, 5 and 7 days post infection. (**A**) Scatterplot of bacterial burden of small intestine and mLNs. (**B**) Scatterplot of bacterial burden of spleen and liver. Each dot represents one mouse, with mean indicated. Data represents three independent experiments (n = 1-4 per experiment) Statistical analysis was performed with Mann-Whitney test, comparing bacterial burden of WT and CCR7$^{-/-}$ mice for each organ and at each time point (*P<0.05; **P<0.01; ***P<0.001).

Figure 3. CCR7 deficiency results in severe inflammation and uncontrolled *Y. pseudotuberculosis* replication. Histopathology of H & E-stained sections of the ileum, mLNs and spleen of WT and CCR7$^{-/-}$ mice orally infected with 10^6 CFU IP32953. Organs were resected on day 3, 5 and 7 post infection. Representative sections of two independent experiments are shown (n = 2-3 per experiment). Bar represents 50 µm for spleen and 100 µm for ileum and mLN. W: white pulp, N: necrosis, Hyp: hyperplasia, B: Bacteria, Neu: neutrophils, Mac: macrophages.

Figure 4. Moderate changes of the immune cell composition in PPs and mLNs. WT and CCR7$^{-/-}$ mice were orally infected with 10^6 CFU IP32953. Of uninfected mice, and on day 1 and 5 post infection single cell suspensions of PPs and mLNs were generated and subjected to flow cytometric analysis. Each dot represents one mouse. Absolute numbers of respective cell populations are depicted. Data represents three independent experiments (n = 1-3 per experiment). Statistical analysis was performed for each time point via unpaired Mann-Whitney test (*P<0.05; **P<0.01).

Figure 5. Dendritic cells and T cells are sustained in WT mice late during *Y. pseudotuberculosis* infection. WT and CCR7$^{-/-}$ were orally infected with 10^6 CFU of IP32953. Single cell suspensions were prepared from mLNs at day 3 and 5 post infection and analysed via flow cytometry. (**A**) Representative dot plot of CD3$^-$CD19$^-$ cells. (**B**) Scatterplot of absolute cell number of CD11c$^+$MHCII$^+$. (**C**) Scatterplot of frequencies of CD3$^+$ cells of total cells. Each dot represents one mouse, with mean indicated. Data represents two to three independent experiments (n = 1-4 per experiment). Statistical analysis was performed by One-way ANOVA with Tukey's post hoc test (*P<0.05; ****P<0.0001).

Figure 6. CCR7 deficiency limits effector T cell cytokine responses in mLNs. (**A-D**) Cytokine profiling supporting T cell differentiation are only upregulated in mLN of WT mice. WT and CCR7$^{-/-}$ were orally infected with 10^6 CFU of *Y. pseudotuberculosis* IP32953. mLNs were dissected of uninfected mice and of

570 infected mice on day 2 and 5 post infection and lysates were analysed for
571 cytokine concentrations normalized to protein concentrations. (**A-B**) Cytokine
572 concentrations in mLNs. Symbols represent mean and standard deviation of
573 two independent experiments (n = 3-4 per experiment). (**C**) Hierachical
574 clustering of cytokine concentration within CCR7$^{-/-}$ and WT mice at day 5 post
575 infection. (**D**) Scatterplot of frequency of RORgT^{+} cells among
576 CD3^{+}CD4^{+} T cells. Statistical analysis was performed for each time point via
577 unpaired Mann-Whitney test (*P<0.05; **P<0.01). (**F**) Survival of WT and
578 Il17af$^{-/-}$ mice upon infection with 10^{7} of *Y. pseudotuberculosis* IP32953
579 followed for fourteen days. Data represents two independent experiments
580 (n = 6-12 per experiment). Statistical analysis was performed using Log-rank
581 (Mantel-Cox) test (*P<0.05).
582

583 ## Supplementary Figure Legends

584 **Supplementary Figure 1.** Sustained upregulation of pro-inflammatory
585 cytokines in PPs of CCR7$^{-/-}$ mice. WT and CCR7$^{-/-}$ mice were orally infected
586 with 10^{6} CFU of *Y. pseudotuberculosis* IP32953. PPs were dissected on day 2
587 and 5 post infection and lysates were analysed for cytokine concentrations
588 normalized to protein concentrations. Symbols represent mean and standard
589 deviation of two independent experiments (n = 3-4 per experiment). Statistical
590 analysis was performed via unpaired Mann-Whitney test (**P<0.01;
591 ***P<0.001).
592

593 **Supplementary Figure 2.** CCR7 deficiency results in maintained systemic
594 inflammation during *Y. pseudotuberculosis* infection**.** Histopathologic scoring

595 of H & E stained sections of the ileum, mLNs, liver and the spleen of mice
596 orally infected with 10^6 CFU IP32953. Organs were resected on day 3, 5 and
597 7 post infection of WT and $CCR7^{-/-}$ mice. (**A**) Bar graph representing the mean
598 of cumulative pathological scores for intestinal tissues and mLNs. (**B**) Bar
599 graph representing the mean of cumulative pathological score for liver and
600 spleen. Data represents two independent experiments (n = 2-3 per experi-
601 ment).
602
603 **Supplementary Figure 3.** Myeloid cell compartment recruited to the spleen
604 after infection with IP32953 in WT or $CCR7^{-/-}$ mice. (**A**) Exemplary gating
605 strategy of splenocytes from uninfected WT mice. (**B**) Scatterplot depicting
606 absolute numbers of indicated cell type.
607 macrophages = $CD49b^-CD19^-CD3^-F4/80^+$,
608 neutrophils = $CD49b^-CD19^-CD3^-Ly6G^+$,
609 monocytes = $CD49b^-CD19^-CD3^-Ly6G^-CD11c^-CD11b^+Ly6C^-$, pro-inflammatory
610 monocytes = $CD49b^-CD19^-CD3^-Ly6G^-CD11c^-CD11b^+Ly6C^+$. Data represents
611 three independent experiments (n = 1-3 per experiment). Statistical analysis
612 was performed via unpaired Mann-Whitney test (*P<0.05)
613
614 **Supplementary Figure 4.** Gating strategy identifying professional dendritic
615 cells. Gating strategy for dendritic cells (DCs) identified as
616 $LiveDead^-Singlets^+Autofluorescence^-CD3^-CD19^-CD11c^+MHCII^+$.

Figure 1

Click here to download Figure Fig. 1.rev1.jpg

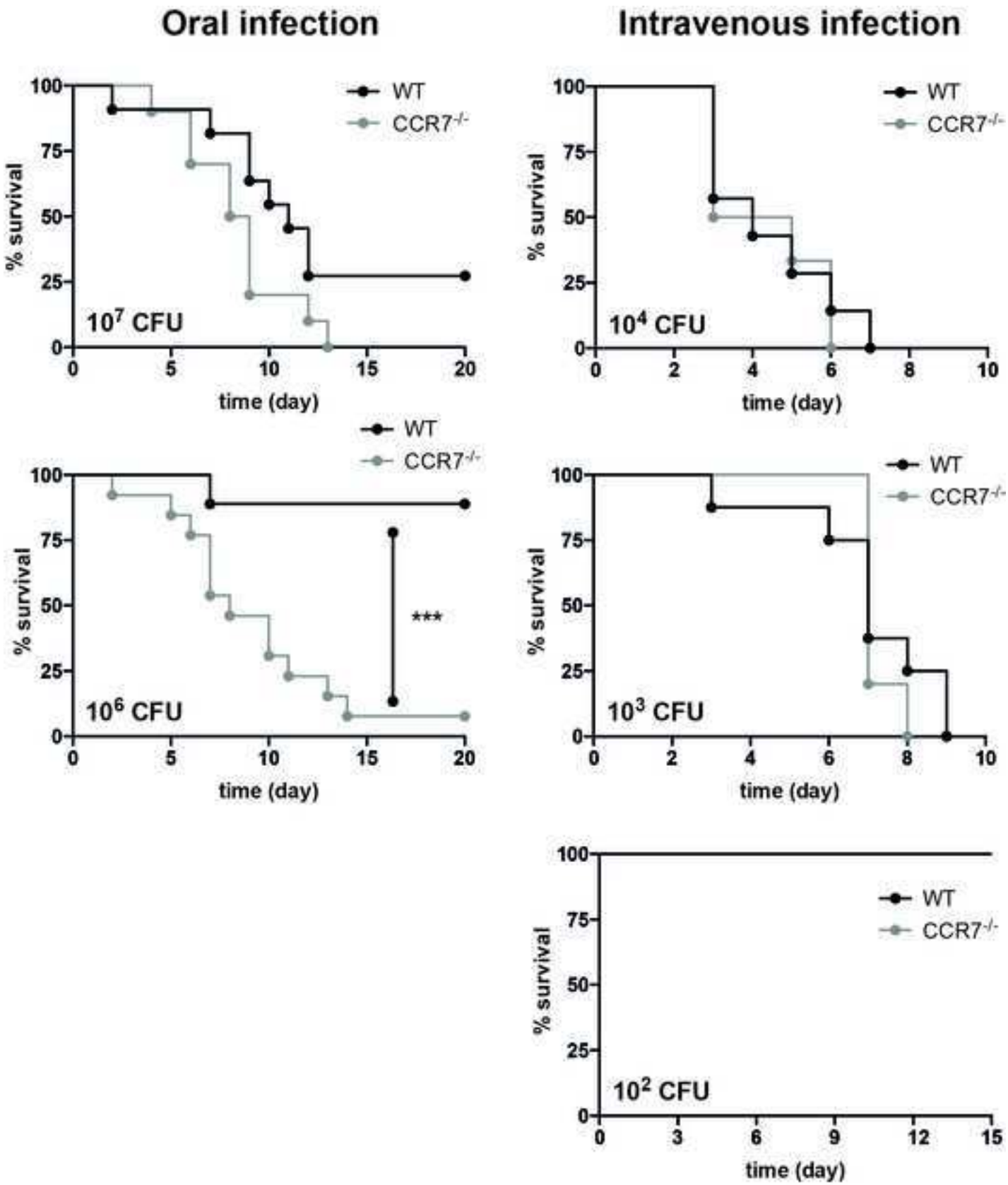

Figure 2

Click here to download Figure Fig. 2.rev1.jpg

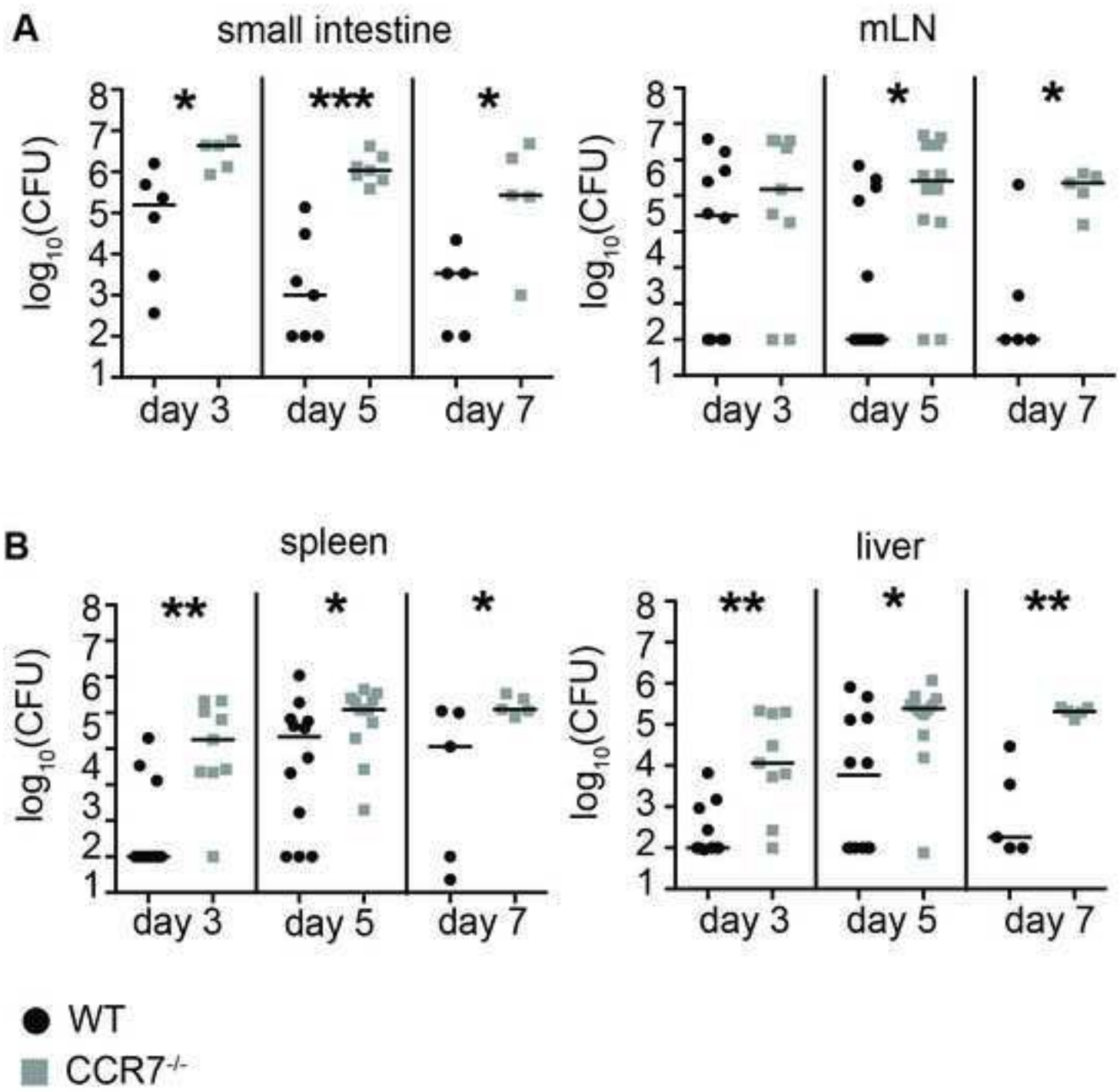

Figure 3

Click here to download Figure Fig. 3.rev1.jpg

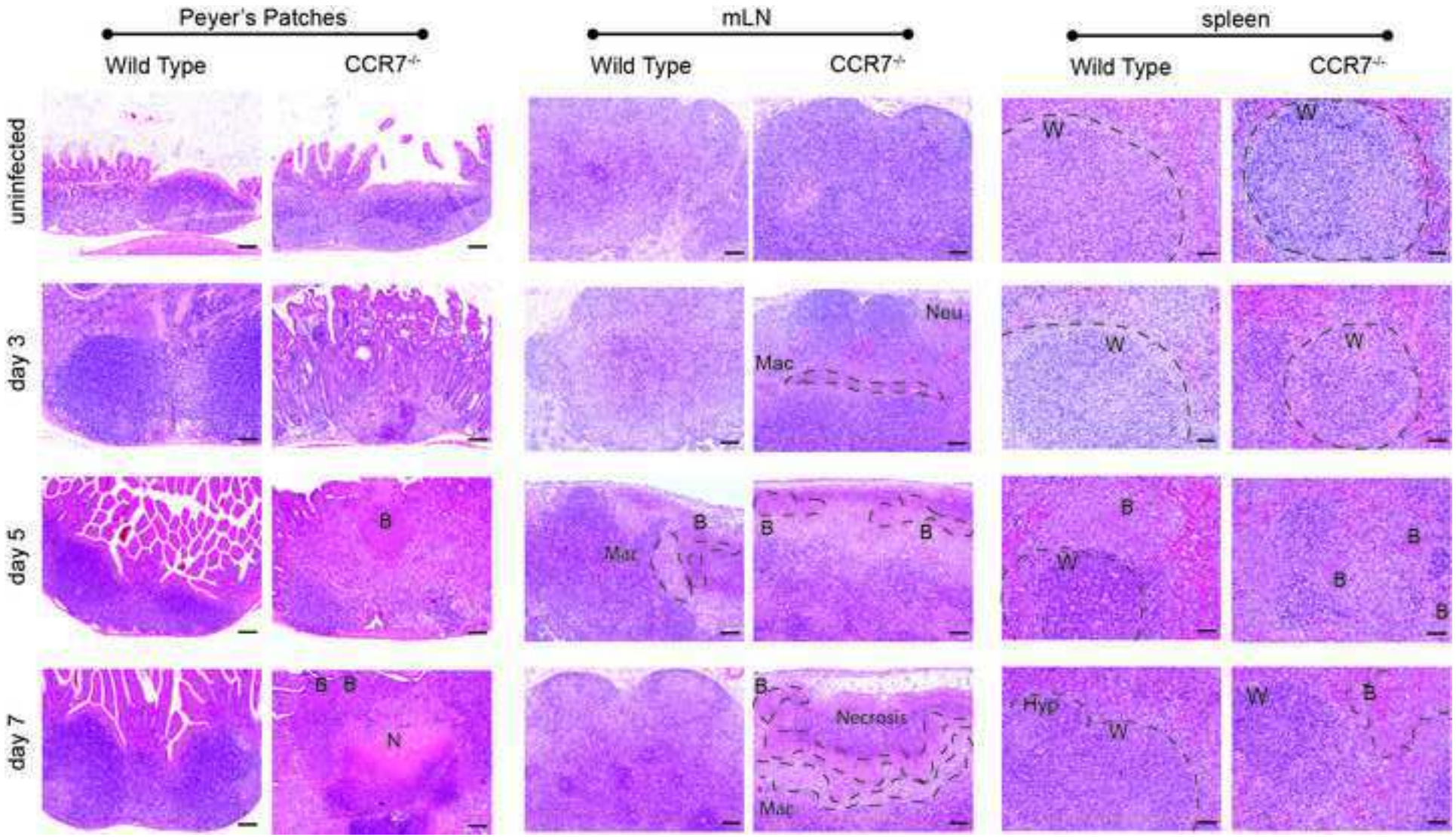

Figure 4

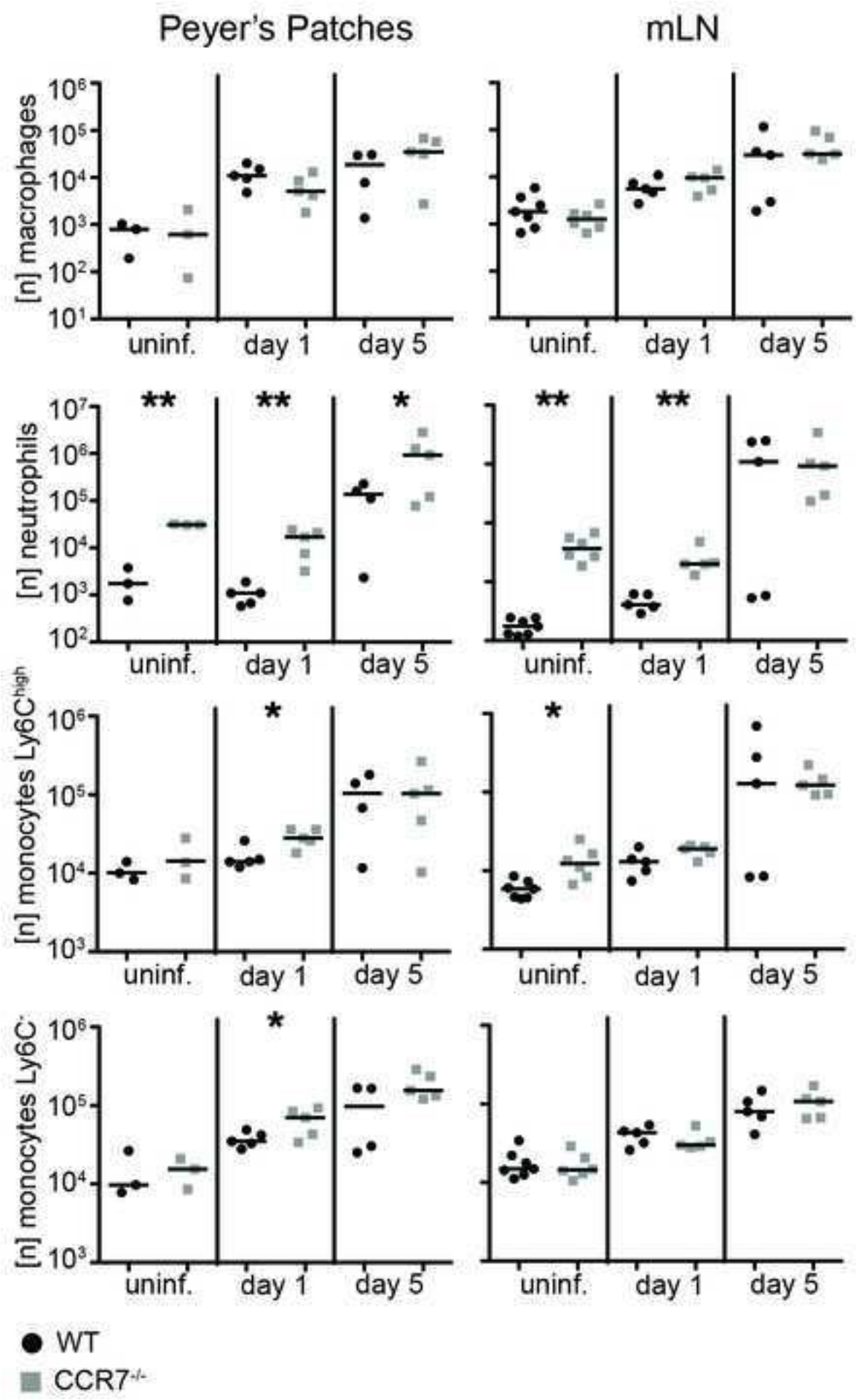

Figure 5

Click here to download Figure Fig. 5.rev1.jpg

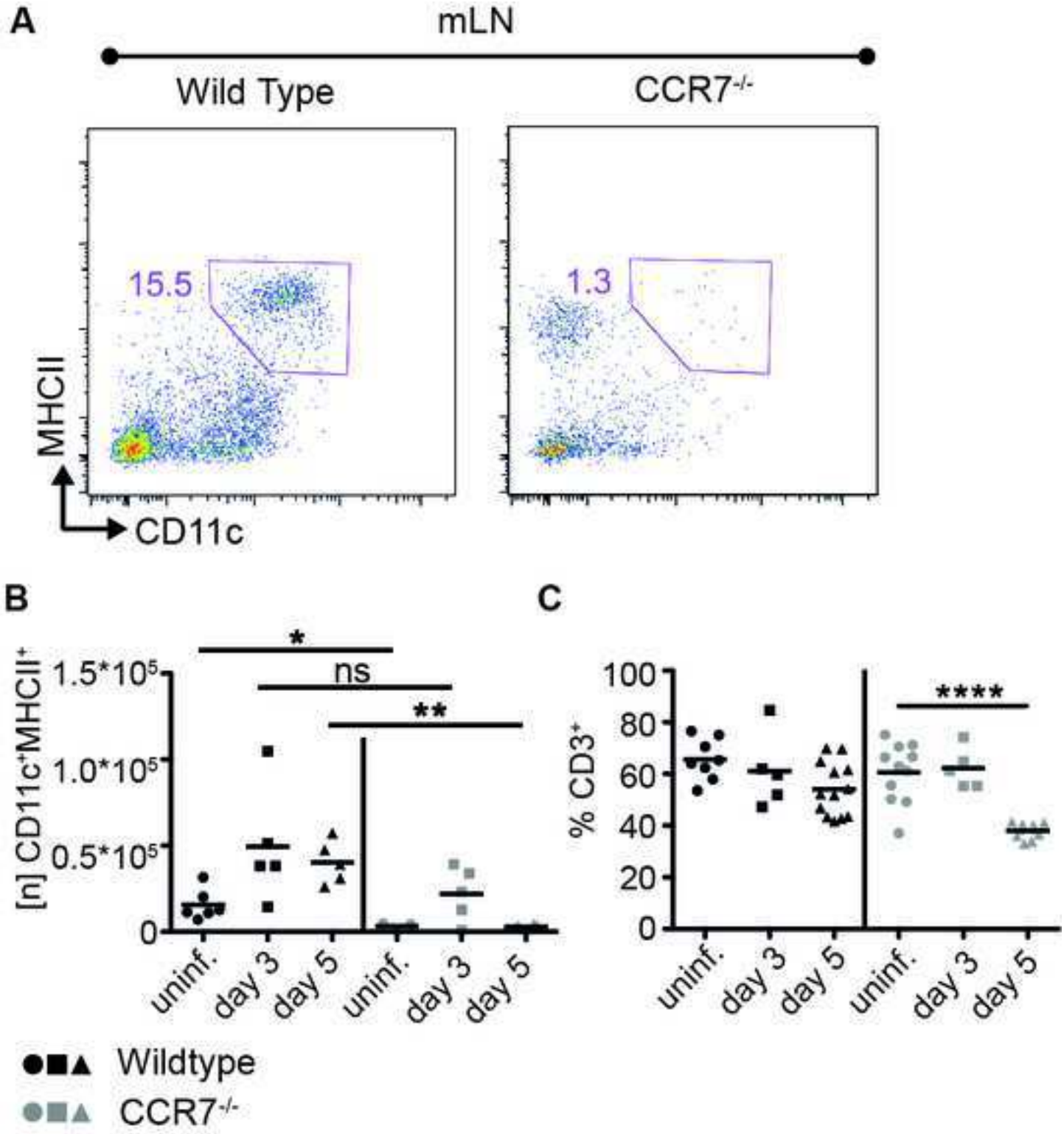

Figure 6

Click here to download Figure Fig. 6.rev.1.jpg

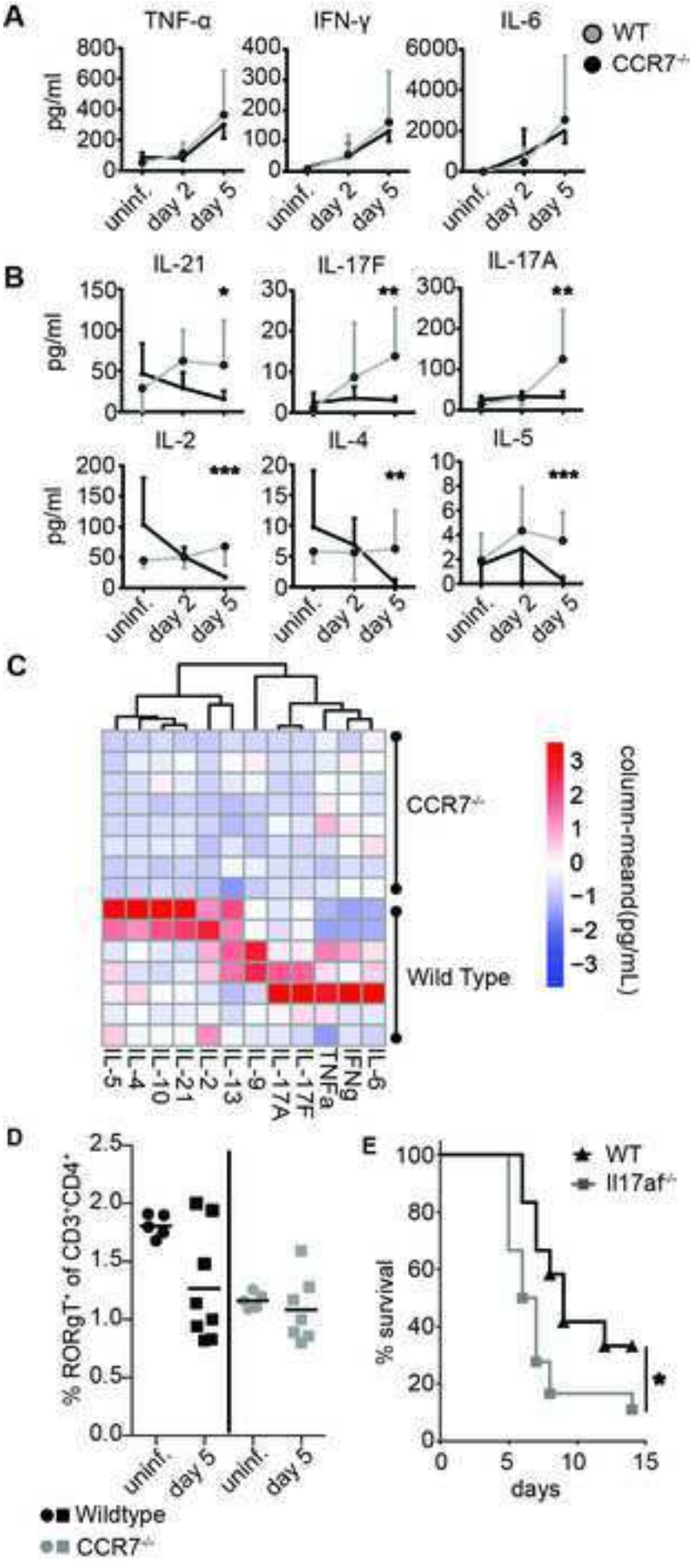

Supplementary Figure S1

Click here to download Figure Fig. S1.jpg

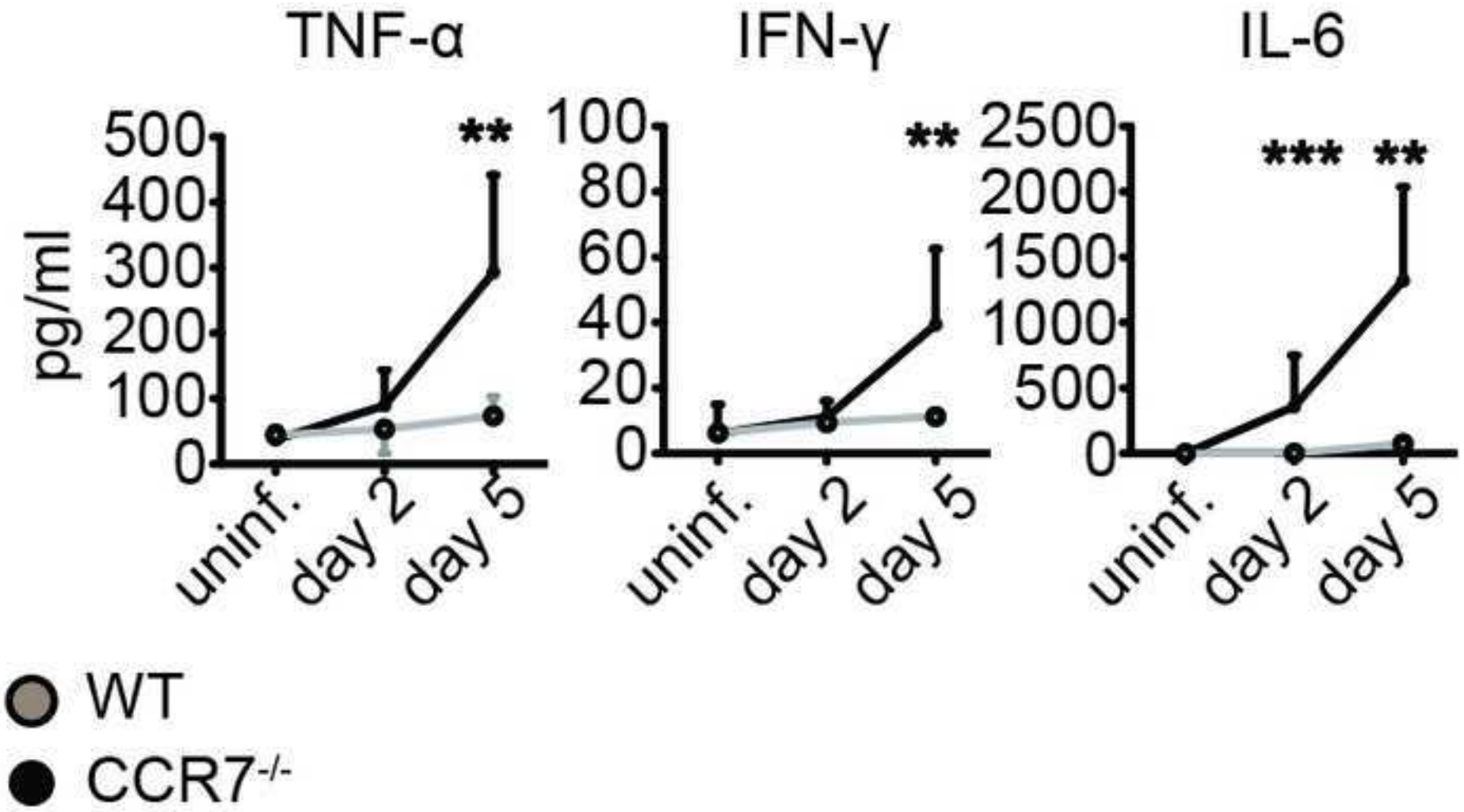

Supplementary Figure S2

Click here to download Figure Fig. S2.jpg

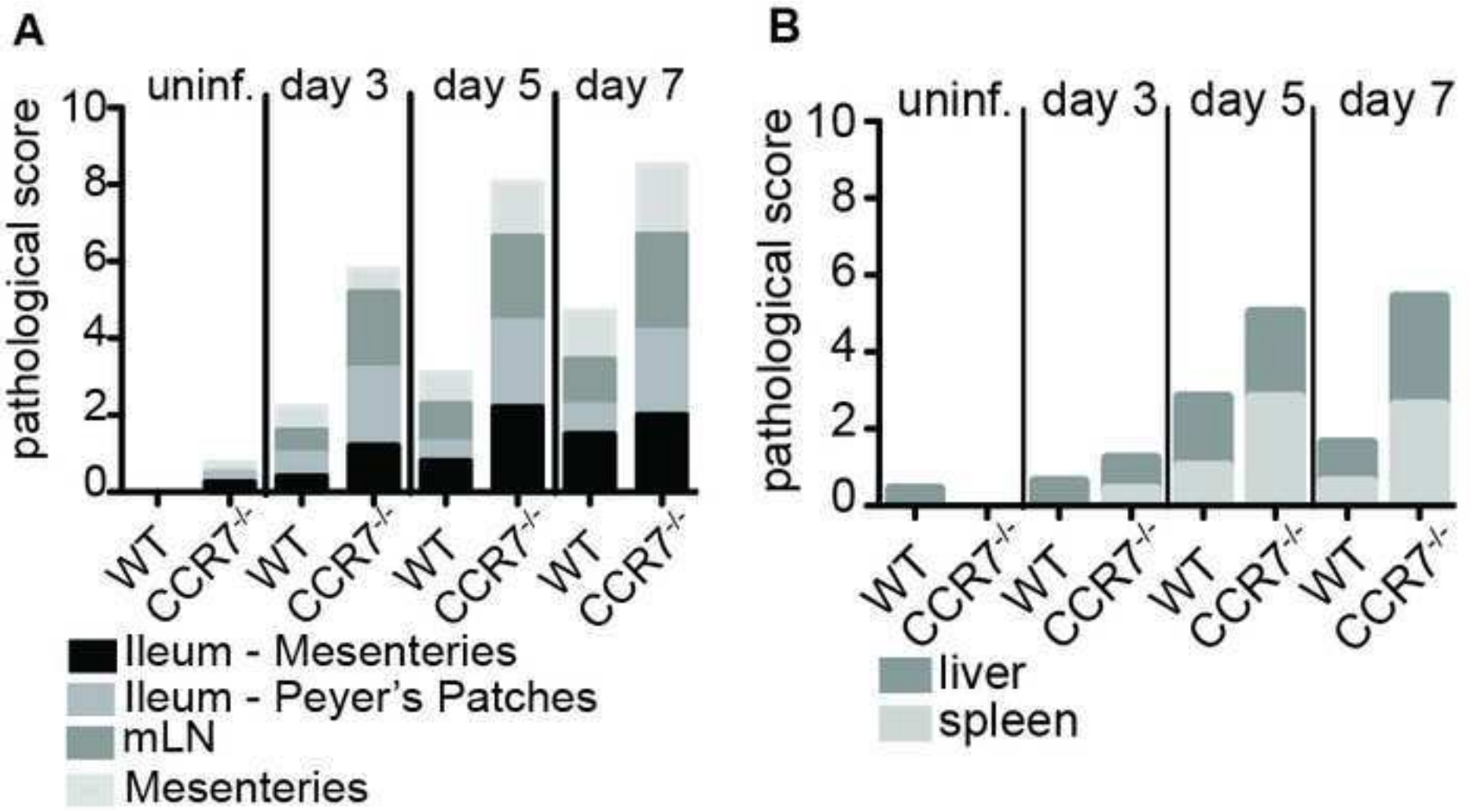

Supplementary Figure S3

Click here to download Figure Fig. S3.jpg

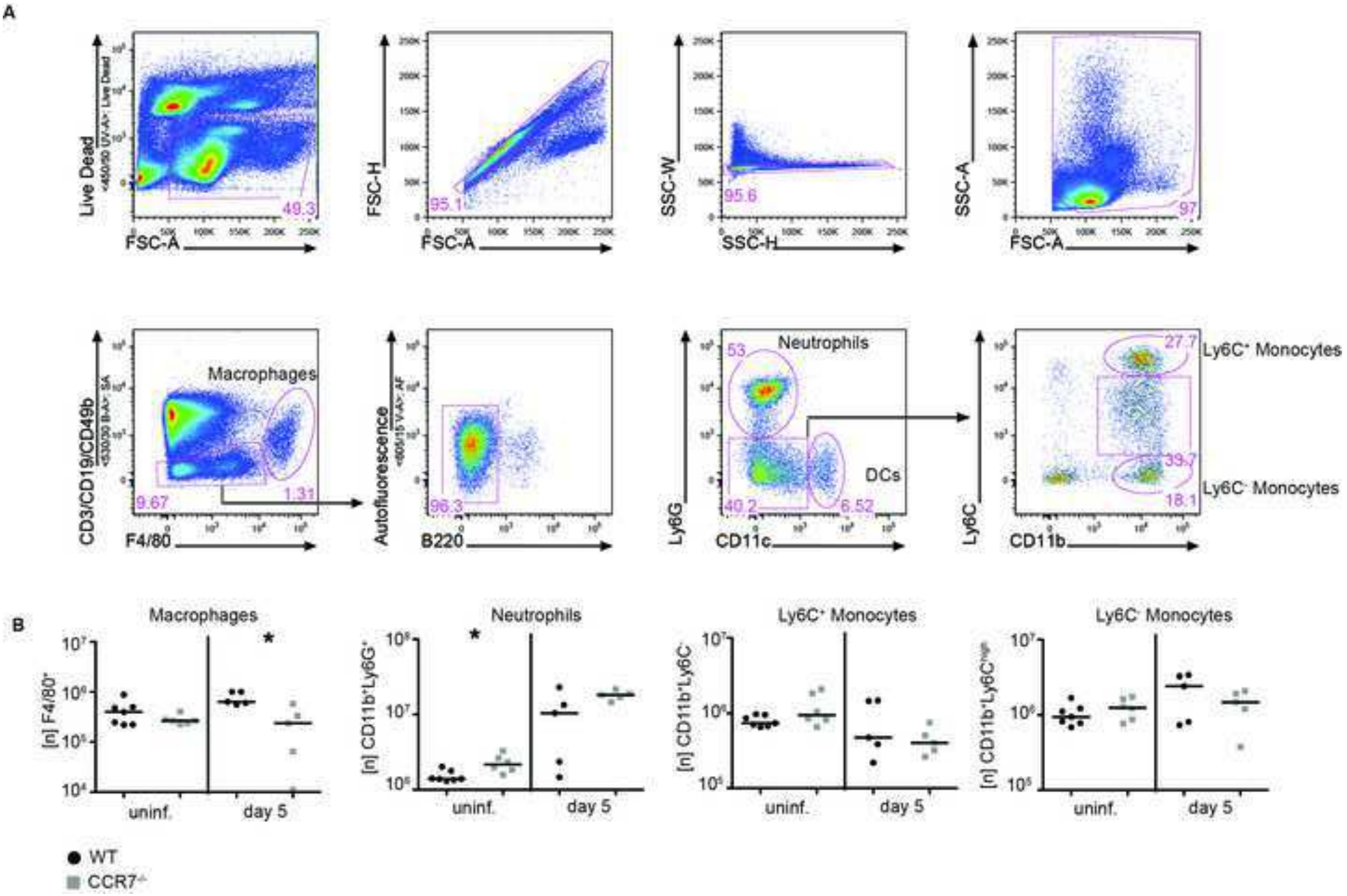

Supplementary Figure S4

Click here to download Figure Fig. S4.jpg

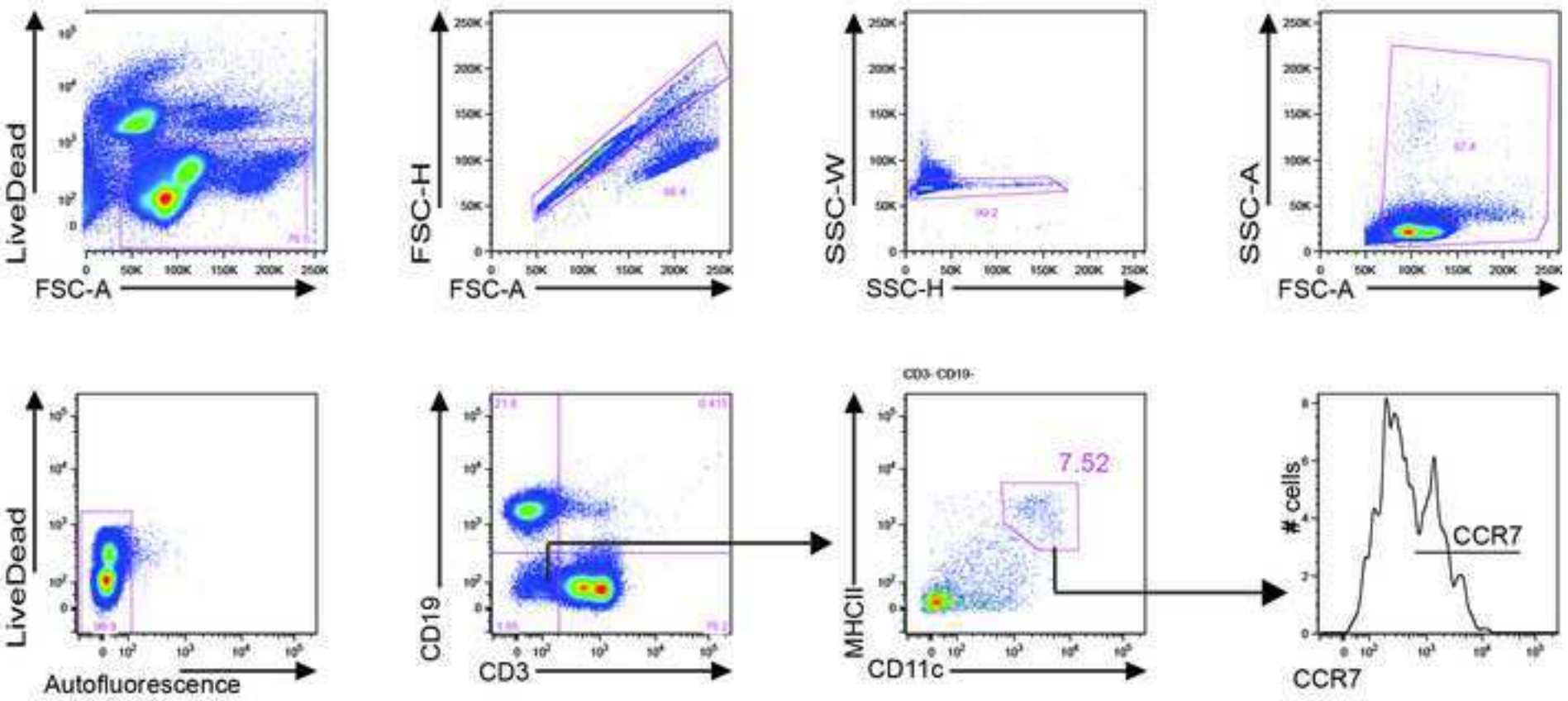

CCR7 deficiency modulates T cell response and increases susceptibility to *Yersinia pseudotuberculosis* infection

Joern Pezoldt, Fabio Pisano, Wiebke Heine, Maria Pasztoi, Maik Rosenheinrich, Aaron M. Nuss, Marina C. Pils, Immo Prinz, Reinhold Förster, Jochen Huehn, Petra Dersch

Supplementary Material

Supplementary Material and Methods

Bacterial strains, media and growth conditions

Cultures of *Y. pseudotuberculosis* were grown at 25°C in Luria-Bertani (LB) broth (Becton Dickinson). For infection experiments, bacteria were grown over night at 25°C, washed twice in sterile PBS and diluted in PBS at the desired concentration.

Histology

Ileum rolled to 'swiss roll', mLNs, liver and spleen were fixed in 4 % neutrally buffered formaldehyde and embedded in paraffin. Sections of 3 µm were stained with hematoxylin/eosin (H & E). Slides were evaluated randomized and blinded to the experimental groups. Severity of inflammation in respective organs was graded as 1 = mild (no inflammation), 2 = moderate (inflammation affecting less than 30 %), 3 = severe (inflammation affecting 30 % to 70 %) or 4 = extreme (inflammation covering more than 70 % of the tissue).

Cytokine expression

PPs and mLNs were aseptically excised and protein lysates were generated with the Bio-Plex Cell Lysis Kit (Bio-Rad). Protein concentrations were determined using the Pierce BCA Protein Assay Kit (Thermo Scientific). Protein lysates were analysed utilizing the Mouse T Helper Cytokine Panel (BioLegend). Samples were acquired with the flow cytometer LSR Fortessa (Becton Dickinson) and analysed with software provided by BioLegend.

Mouse infection

C57BL/6 (WT), isogenic B6.129P2(C)-Ccr7tm1Rfor/J (CCR7$^{-/-}$) and B6.Il17a/Il17ftm1.1Impr (IL17af$^{-/-}$) mice were bred at the animal facility of the Helmholtz Centre for Infection Research, Braunschweig. All animals were housed under specific-pathogen free (SPF) conditions and food and water were given *ad libitum*. Fourteen hours prior to infection of 10-14 weeks old female mice, food was removed and added back immediately after infection. Oral infections were performed intragastrically using a ball-tipped gavage needle, while intravenous (*i.v.*) infections were performed via the lateral tail vein. For organ burden, the small intestine, mLNs, liver and spleen were aseptically resected and colony forming units (CFUs) were determined as described previously (1). In survival assays, mice were infected orally with different *Y. pseudotuberculosis* CFUs in 200 µl PBS, and intravenously in 100 µl PBS. Infected animals were monitored daily for up to 20 days or until the surviving individuals displayed full recovery.

Flow cytometry

On day 1, 3 and 5 post infection, PPs, mLNs and spleen were isolated and single cell suspensions generated. Cells were resuspended in FACS-buffer (0.05 % BSA in

PBS) and total cell number was determined via Beckman Coulter Counter Z2. Dead cells were identified via live/dead fixable blue staining (Invitrogen). Fc-receptors were blocked with α-mouse CD16/CD32 (cl.93). Antibodies against CD3:PerCP-Cy5.5 (17A2), CD3e:Biotin (145-2C11), CD11b:eFluor450 (M1/70), CD11c:PE-Cy7 (N418), CD11c:APC-eFluor780 (N418), CD19:FITC (6D5), CD19:Biotin (eBio1D3), CD45R:PerCP-Cy5.5 (RA3-6B2), CD49b:Biotin (DX5), MHCII:AlexaFluor-700 (M5/114.15.2), CCR7:BV421 (4B12), Streptavidin:FITC, F4/80:PE (BM8), Ly6G:PE-Cy7 (1A8) and Ly6C:APC (HK1.4) were purchased from eBioscience, Becton Dickinson and BioLegend. Data were collected with flow cytometer LSR Fortessa (BD Biosciences), and analysed with FlowJo (Treestar).

Statistical analysis

Flow cytometry data were analysed via one-way ANOVA followed by Tukey's multiple comparison tests. Survival curves were compared using the Log-Rank (Mantel-Cox) test. Bacterial burdens in the organs and cytokine data were compared using the Mann-Whitney test. Statistical analysis was performed using GraphPadPrism 5 (GraphPad Software, La Jolla, USA). Heatmaps were generated with *R* utilizing the package *pheatmap*.

References:

1. Schweer J*, et al.* (2013) The cytotoxic necrotizing factor of *Yersinia pseudotuberculosis* (CNF_Y) enhances inflammation and Yop delivery during infection by activation of Rho GTPases. *PLoS Pathog* 9(11):e1003746.